Engineering Geology 230 (2017) 77–83

Contents lists available at ScienceDirect

Engineering Geology

journal homepage: www.elsevier.com/locate/enggeo

# Clarification of capillary rise in dry sand

Robert Hird*, Malcolm D. Bolton

*Geotechnical and Environmental Group, Department of Engineering, University of Cambridge, Cambridge CB2 1PZ, UK*

ARTICLE INFO

*Keywords:*
Capillary rise
Dry sand
Rising head tests
Young-Laplace

ABSTRACT

The extent of capillary rise into initially dry granular soil, that is exposed at the surface and subjected to wetting at the base, is not easy to predict. Simple rising head column experiments were performed using pure water in medium-grained poorly graded and unconsolidated sand to shed light on the extent to which water rises in initially dry soil and its distribution. Rising head experiments have been conducted in initially dry sand to explore these phenomena in columns instrumented with Time Domain Reflectometry (TDR) probes, the data from which are compared with water contents ultimately found gravimetrically from sample slices. Water was found to reach much higher than theoretical estimates based on an equivalent capillary tube, suggesting that capillary rise is responsible for fluid transport well into the zone of unsaturated soil above the saturated capillary zone. This remained the case even when the sand was subjected to strong rates of evaporation at its surface. This study challenges the conventional understanding of capillary rise in unsaturated soil and has particular relevance in desert soils subject to rapid evaporation.

### List of symbols

| | |
|---|---|
| CF | capillary fringe |
| d | pore diameter |
| $D_{10}$ | particle size at which 10% of particles are smaller |
| g | acceleration due to gravity |
| GWL | groundwater level |
| $h_c$ | capillary height |
| $h_{max}$ | maximum height of capillary rise |
| ID | internal diameter |
| $k_s$ | hydraulic conductivity |
| n | porosity |
| OD | outer diameter |
| RH | relative humidity |
| S | saturation |
| SWCC | soil water characteristic curve |
| t | time |
| T | surface tension |
| TDR | time domain reflectometer |
| $\alpha$ | contact angle |
| $\eta$ | dynamic viscosity of water |
| $\nu$ | kinematic viscosity of water |
| $\rho_w$ | density of water |

## 1. Introduction

The possible extent of capillary rise in initially dry granular soil, subject to wetting at the base, and exposed at the surface, needs clarifying. The current understanding of the moisture (soil water) distribution focuses on the fluid remaining in soil pores following the downward drainage of previously saturated soil, such as in pressure-plate tests.

The extent to which fluid can rise above the water table is important in the study of solute transport. This is especially true for low-lying desert soils with shallow groundwater levels, which are fed from below by capillarity but which are subject to high rates of evaporation at their surface associated with solar radiation and diurnal changes in air relative humidity. These soils are typically granular, poorly graded and unconsolidated having been lain down largely through aeolian and maritime processes. To understand the vertical extent and distribution of pure water undergoing capillary rise in dry medium grained sand a number of rising-head column experiments have been conducted. In each experiment the groundwater table remains static and no surface infiltration takes place. The effect of changing the relative humidity of the air above the surface of the sample and the temperature of the entire sample and is explored and compared to theoretical estimates.

## 2. Background

The conventional understanding of the vadose zone is shown in

* Corresponding author.
*E-mail address:* rh500@cantab.net (R. Hird).

http://dx.doi.org/10.1016/j.enggeo.2017.09.023
Received 14 February 2017; Received in revised form 26 September 2017; Accepted 26 September 2017
Available online 28 September 2017
0013-7952/ © 2017 Elsevier B.V. All rights reserved.

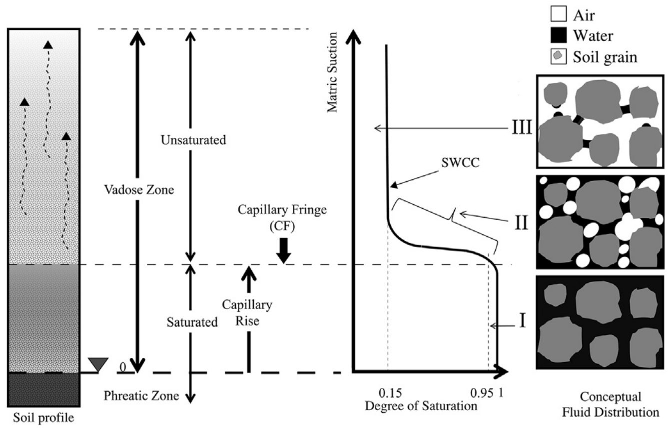


**Fig. 1.** Conventional understanding of the vadose zone suction and degree of saturation, derived by draining water from a saturated soil.

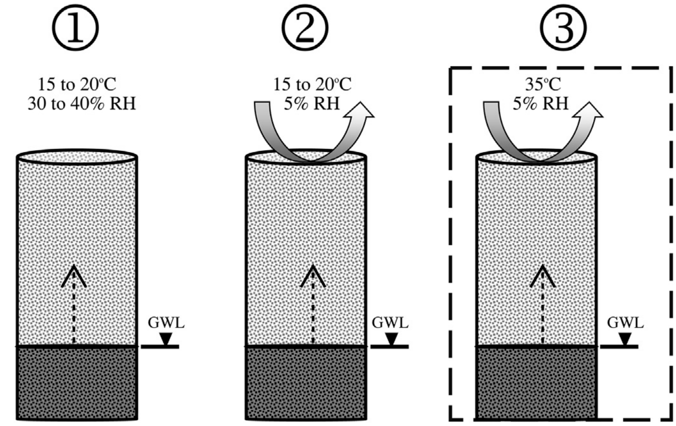


**Fig. 2.** Experimental conditions surrounding each rising head test. 1 Variable temperature and relative humidity; 2 Variable temperature but with low humidity air at the surface; 3 Constant elevated temperature and low humidity air at the surface.

Fig. 1. The groundwater table or phreatic surface marks a surface with the pore fluid at atmospheric pressure, and the phreatic zone beneath is assumed to remain saturated. The vadose zone lies between the phreatic zone and the soil surface, and contains soil that is increasingly unsaturated at higher elevations. The capillary rise of water takes place above the phreatic surface, the extent of which is determined by the soil pore size, and fluid properties including surface tension.

The top of the capillary fringe marks the extent of that part of the capillary rise where the fluid can be continuous and the soil can remain saturated. A typical representation of a soil water characteristic curve (SWCC) is also presented in Fig. 1 showing the relationship between matric suction generated by the pressure difference between water, fluid and air and its degree of saturation. These curves are typically generated by measuring capillary pressure during soil drainage (e.g. using the porous plate technique) or by curve fitting from soil models (e.g. Van Genuchten, 1980).

Three separate zones are conventionally recognised within the vadose zone using the measurement of the SWCC curve, as shown in Fig. 1. The lowest suction is applicable to the capillary zone (marked I in Fig. 1) which is sometimes defined as lying between a degree of saturation of 1 and 0.95 (Robert and Soga, 2010) suggesting either saturation or near-saturation with discontinuous air bubbles. Fredlund and Rahardjo (1993) however, suggest that this zone should be free of air bubbles, which may be expected to have dissolved in the groundwater. If the suction exceeds that of the capillary pressure, air can enter from above or bubbles can resist water rising from below. This distinguishes the lower boundary of the intermediate funicular zone II in Fig. 1 within which both air and water phases can be continuous. The upper boundary of zone II represents the point at which the suction corresponds to fluid menisci of such high curvature that isolated water droplets can only exist as pendular bridges between grains, the remaining void space comprising a continuous air phase. This pendular moisture zone is marked III in Fig. 1. The transition from zone II to zone III depends on the grain sizes and is considered relatively sharp (Silliman et al., 2002); it has been taken at 0.15 degree of saturation in Fig. 1 from the observations of Robert and Soga (2010) for Cornell sand. The terms pendular moisture regime for residual moisture trapped at grain contacts, and funicular moisture regime where water droplets coalesce into continuous filaments, were coined by Haines (1930). A cartoon next to the SWCC in Fig. 1 shows the possible arrangement within each moisture regime. This arrangement derived from experiments conducted by drying saturated soil will be used to understand fluid distribution by wetting from below.

## 3. Equipment, materials and experimental procedures

Rising head tests were performed to determine the height reached by water in three different scenarios as shown in Fig. 2. Some previous references of rising head tests into dry granular media through experimental means involve the covering of the surface to control internal conditions (e.g. Yang et al., 2004; Feia et al., 2014) to ensure an equilibrium condition is reached between the water and air in the pores resulting in a static capillary fringe. However this does not necessarily consider real conditions as soil above the water table is invariably exposed to ambient conditions. This potential variability in surface conditions and the effect it has on the height of the capillary fringe is explored by conducting tests 1 and 2 at variable temperature and different relative humidity compared with constant elevated temperature and relative humidity conditions in test 3. The groundwater level was maintained at a constant elevation above the base of each column, and tests carried out in triplicate. The water content was determined by gravimetric analysis of samples.

Tests were performed in clear acrylic columns (300 mm long, 100 mm ID) with a filter placed at the base of the columns to retain the sand. The dimensions and features of the column are presented in Fig. 3(a). Circumferential markings were made at 30 mm spacing on the wall of the column to guide soil extraction (Fig. 3(b)). In experiments 2 and 3, air of low relative humidity was allowed to pass over the surface at the top of the column (Fig. 3(c)). The low relative humidity air stream and elevated temperature were to simulate arid field conditions. Relative humidity was monitored using Sensirion© chips (Type SHT71) which had an accuracy of ± 3% RH.

In addition, for experiment 3, constant temperature was supplied by means of an incubator (Genlabs, UK) which had a temperature accuracy of ± 0.5 °C at 5 °C above ambient temperature.

Washed, air-dried Fraction D sand (supplied by the Davis Ball Group, Cambridge, UK) was placed into the columns in layers whilst being vibrated on a table to ensure a uniform density. The characteristics of the sand, based upon six repeated sieve tests, are shown in Fig. 4 and the properties of each test in Table 1. The sand-filled columns were stood in a tray of water with its level maintained until the capillary height had stabilised (determined by the colour difference between wet and dry sand) after about 200 h. Soil slices measuring 30 mm thickness were then quickly removed to determine the moisture content.

The measurement of moisture contents in sand by the extraction of sample layers may be subject to error if there is any loss of fluid by drainage during their removal, and only provides the average fluid content of each soil slice. Instead time domain reflectometer (TDR) probes placed horizontally can be employed to infer the local moisture

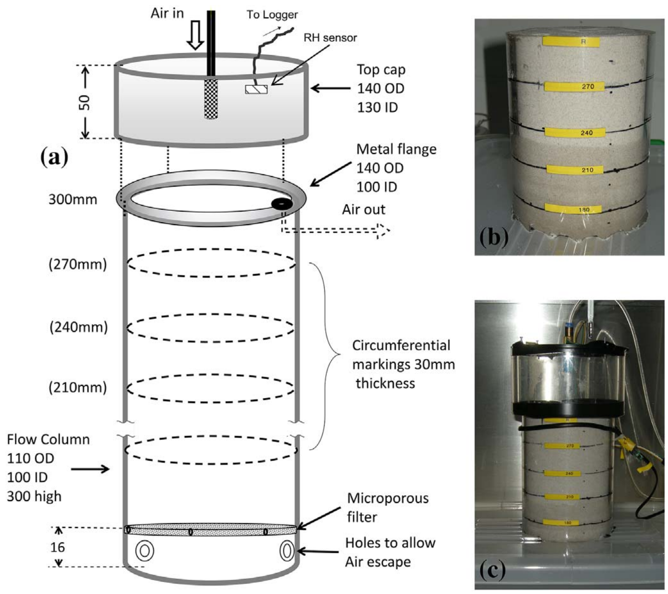


**Fig. 3.** Configuration of columns to determine the capillary rise by rising head; (a) dimensions and features of the column; (b) capillary rise in Test 1; (c) capillary rise in Test 3 sat inside an incubator.

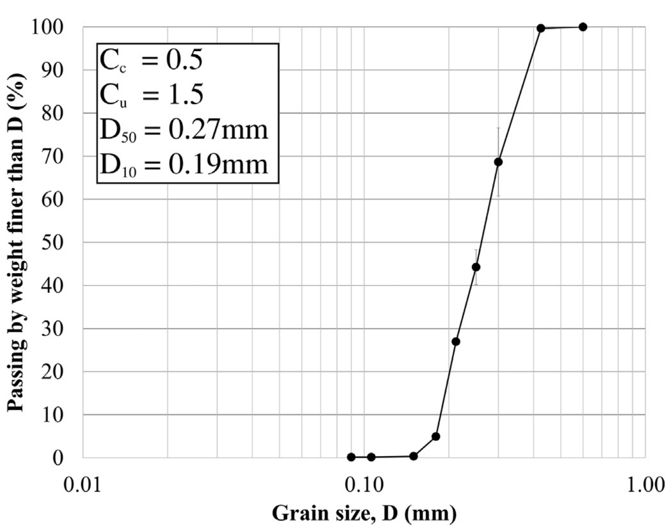


**Fig. 4.** Grading curve for Fraction D sand.

**Table 1**
Characteristics of rising head tests for moisture content determination.

| Parameter | Units | Test 1 | Test 2 | Test 3 |
|---|---|---|---|---|
| Dry density | g/cm$^3$ | 1.68 | 1.68 | 1.68 |
| Porosity | – | 0.37 | 0.37 | 0.37 |
| Airflow rate | l/min | – | 10 | 10 |
| Temperature | °C | 15–20 | 15–20 | 35 |
| RH at surface | % | 30–40 | 5 | 5 |

content as the water front rises through the soil profile (Jones et al., 2002). TDR probes measure dielectric permittivity which is empirically related to volumetric water content (Topp et al., 1980). TDR probes have previously been documented in geotechnical applications to measure volumetric water content and degree of saturation in unsaturated soils (e.g. Krisdani et al., 2008; Lehmann et al., 2013; Lucas et al., 2015).

Five TDR probes situated in the top half of the column were used to detect volumetric water content during rising head tests. Each probe

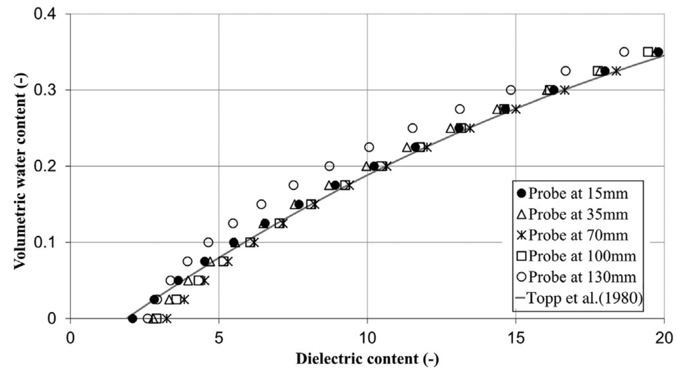


**Fig. 5.** Dielectric constant versus volumetric water content relationship for Fraction D sand compared with the same relationship determined by Topp et al. (1980).

was first calibrated in air and water to determine the offset (end of cable and start of the immersed probes) and then each separately placed horizontally in a modified Tempe cell to determine the dielectric constant – volumetric water relationship in Fraction D sand. Dielectric constant measurements were made at regular intervals using a Campbell Scientific TDR100 at different volumetric water contents. Fig. 5 presents the volumetric water content and dielectric constant for each probe compared to that derived by Topp et al. (1980). Small variations in in probes at 15 mm, 35 mm, 50 mm and 100 mm are due to the dissimilar measurement times and the probe at 130 mm is shown to over predict the volumetric water content by about 15% compared to the relationship by Topp et al. (1980). However the volumetric water content –dielectric constant in this experiment is unique to each probe and has not been corrected to compensate to any published reference.

To allow for the placement of the 50 mm TDR probes horizontally in the test column, holes were drilled into the side of the acrylic column at five elevations as shown in Fig. 6(a). The orientation of the TDR probe in the column is shown in Fig. 6(b). An instrumented column of sand under test is shown in Fig. 6(c). Placement of Fraction D sand within the instrumented columns was repeated as for non-instrumented columns.

Tests using TDR probes were conducted to determine the effect of temperature change on the degree of saturation above the capillary fringe; the properties of each test (labelled as A and B) are presented in Table 2.

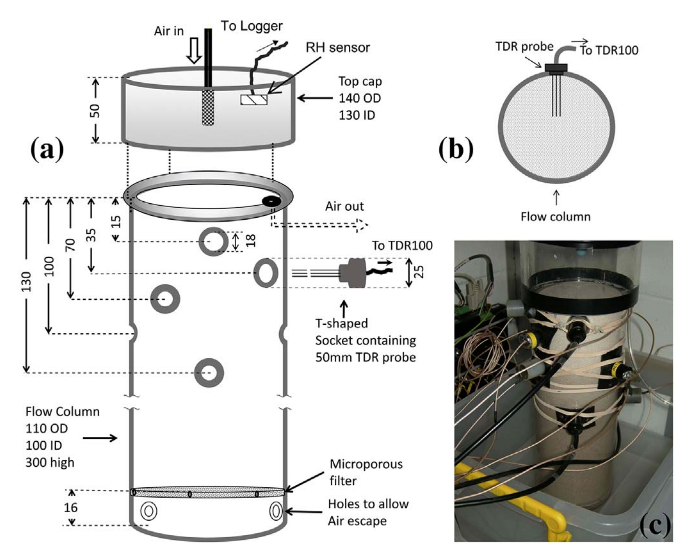


**Fig. 6.** Configuration of columns to determine the capillary rise by rising head with TDR probes; (a) dimensions and features of the column; (b) arrangement of the TDR probe in the column; (c) capillary rise in Test A.

**Table 2**
Characteristics of rising head tests using TDR probes.

| Parameter | Units | Test A | Test B |
|---|---|---|---|
| Dry density | g/cm$^3$ | 1.68 | 1.69 |
| Porosity | – | 0.37 | 0.36 |
| Airflow rate | l/min | 10 | 10 |
| Temperature | °C | 15–20 | 35 |
| RH at surface | % | 5 | 5 |
| GWL (measured from top of the sand surface) | mm | 281 | 279 |

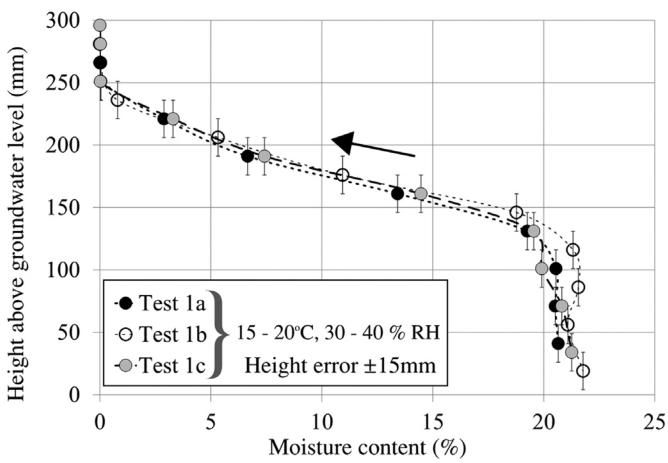


**Fig. 7.** Moisture content curves for rising head tests on a column of Fraction D sand using pure water for Test 1. Arrow indicates direction of water flow.

## 4. Results

### 4.1. Experimental measure of capillary rise height

Fig. 7 presents the soil moisture curve above the groundwater level for Test 1. The data of tests 1a, 1b and 1c are very consistent considering that they were obtained by sampling and weighings. They are also presented as averages in Fig. 8 along with experiments 2 and 3. The height reached by the water is summarised for each test in Table 3.

The experiments were repeated for low relative humidity surface conditions. To convert dielectric constant to fluid saturation it is necessary to first determine the volumetric water content relationship (which is unique to each probe and presented in Fig. 5) and take into account the sample porosity. Fig. 9 presents the increase of volumetric water content with time with the same data but presented as degree of saturation in Fig. 10. To compare the data from gravimetric analysis and TDR probes for the test case where the sample was maintained at 35 °C and subjected to a surface humidity of 5%, data from Fig. 8 (Test 3) and Fig. 10 (Test B) were combined as shown in Fig. 11. The plot shows that the TDR derived values of water distribution, in the form of degree of saturation, represent the upper part of the wetting curve. The small differences in degree of saturation compared to that shown by the moisture content curve is attributed to sampling errors, 0.01 difference in porosity between test 3 and test B, and at 130 mm, the errors associated with dielectric to volumetric water content relationship (see Fig. 5).

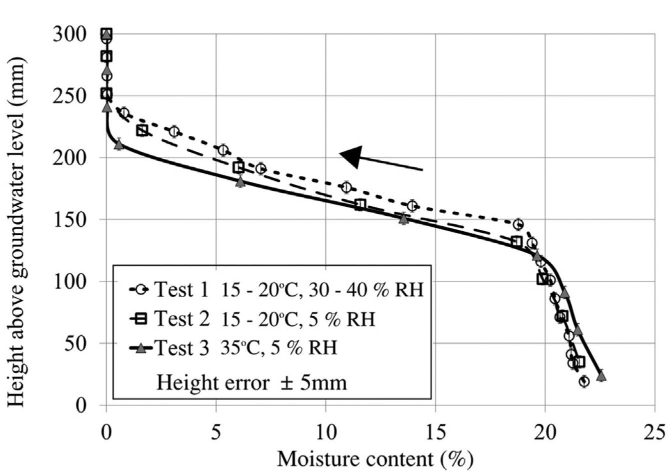


**Fig. 8.** Moisture content curves for rising head tests on a column of Fraction D sand using pure water for Test 1, Test 2 and Test 3 (plotted as averages of sample weighings). Arrow indicates direction of water flow.

**Table 3**
Height reached by water above the phreatic surface.

| Test | Height of water above the phreatic surface (mm) |
|---|---|
| 1 | 252 |
| 2 | 236 |
| 3 | 217 |

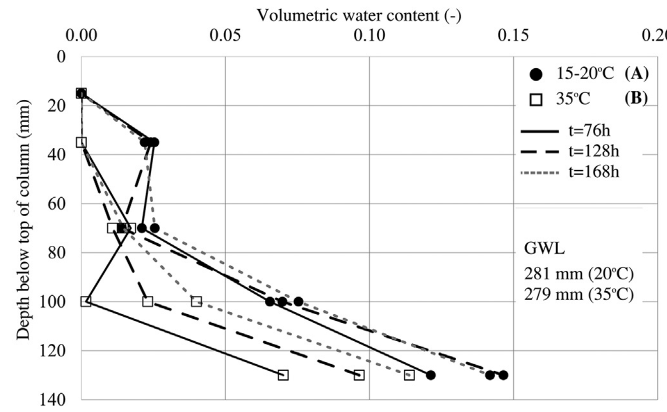


**Fig. 9.** Change in volumetric water content up to 130 mm depth below the sand surface which is maintained at 5% relative humidity.

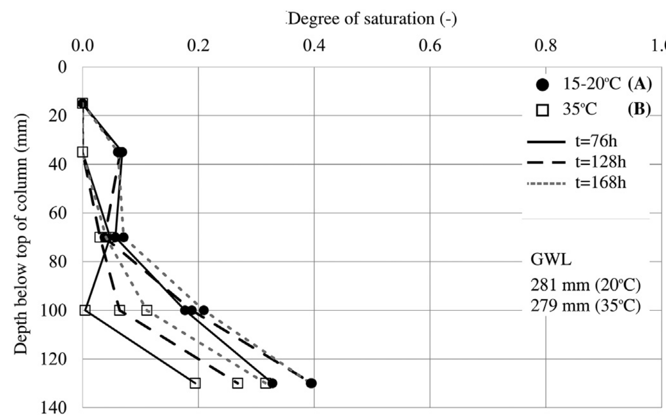


**Fig. 10.** Change in degree of saturation up to 130 mm depth below the sand surface which is maintained at 5% relative humidity.

### 4.2. Theoretical estimates of capillary rise

The capillary height $h_c$ of pure water in the ground is often estimated in geotechnics by considering soil as equivalent to a bunch of capillary tubes and using the Young-Laplace Eq. (1). The equivalent pore diameter d in Eq. (1) is often taken as the $D_{10}$ grainsize (Terzaghi and Peck, 1964). Using $D_{10}$ = 0.19 mm for the Fraction D silica sand (shown in Fig. 4), with water properties at 20 °C taken as surface

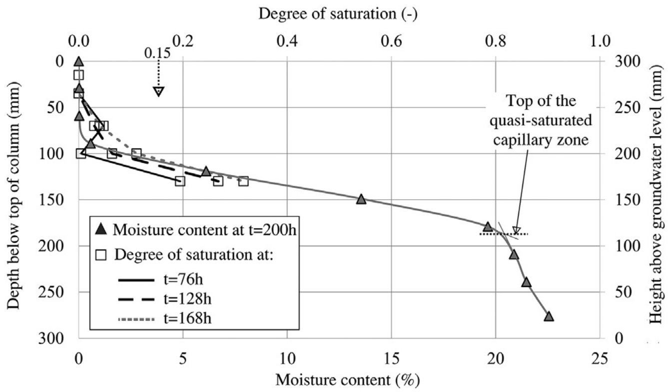


**Fig. 11.** Relationship between moisture content from soil slices and saturation determined by TDR at 35° C when sand is subjected to 5% relative humidity at the surface.

tension T = 72.75 mN/m (Vargaftik et al., 1983), density $\rho_w$ = 1000 kg/m$^3$, the capillary height $h_c$ is estimated as 156 mm. The equivalent values at 35 °C are 70.41 mN/m (Vargaftik et al., 1983) for surface tension and a density of 994 kg/m$^3$ (Tanaka et al., 2001) for pure water which relate to a capillary height of 152 mm. These estimates assume full wettability between the rising fluid and the sand grains (i.e. contact angle $\alpha$ = 0).

$$h_c = \frac{4T\cos\alpha}{d\rho_w g} \tag{1}$$

It is tacitly assumed that this estimate relates to the maximum elevation of the saturated capillary front above the groundwater table. It must also be treated as approximate since there is no accepted density relation, whereas it is self-evident that a closer packing of grains should lead to tighter pore spaces, a reduced effective pore diameter, and a higher capillary zone. Similarly, the presence of air in pores above the saturated capillary zone must also tend to constrict the water-filled channels, and this too will the permit further capillary rise seen in Fig. 11.

Both capillary rise and hydraulic conductivity are based theoretically on an equivalent pore diameter, which is squared in the case of hydraulic conductivity. Accordingly, Liu et al. (2014) predicted the fluid rise in granular soil by considering hydraulic conductivity, expanding on work undertaken previously by Malik et al. (1984) and others. The maximum height of capillary rise ($h_{max}$) was therefore suggested as:

$$h_{max} = \frac{Tn}{\sqrt{2\eta\rho_w g k_s}}\cos\alpha + (1-n)h_c \tag{2}$$

where $\eta$ is the dynamic viscosity of water, $k_s$ is the hydraulic conductivity, $h_c$ is the height of the saturated capillary fringe, n is the porosity and $\alpha$ is the advancing contact angle. This measurement was recognised by Liu et al. (2014) to be approximate in order to obtain "a quick estimation". In particular, the equivalent pore radius for flow was taken as constant throughout the wetted zone whereas it must reduce in the unsaturated region where air invades the larger pores and reduces the area available for flow; and while the hydraulic gradient was also taken to be constant over the wetted height, the greater resistance to flow in the unsaturated zone will actually lead to a steeper pressure gradient within it.

If Eq. (2) is used, notwithstanding the simplicities involved in its derivation, an independent estimate of $h_{max}$ can be obtained if the saturated permeability $k_s$ can also be estimated. The Kozeny-Carman equation (Carman, 1937; Bear, 1972) is widely accepted:

$$k_s = 8.3\ 10^{-3}\frac{g}{\nu}D_{10}^2\left[\frac{n^3}{(1-n)^2}\right] \tag{3}$$

where $\nu$ is the kinematic viscosity which is 7.25 × 10$^{-7}$ m$^2$/s at 35 °C (Venard and Street, 1975). The permeability $k_s$ in this experiment can then be estimated as 4.62 × 10$^{-4}$ m/s using the measured porosity n of 0.36. Using Eq. (2) with the dynamic viscosity of water at 35 °C as 0.69 mPa.s (Venard and Street, 1975), along with a measured $h_c$ of 110 mm (± 10 mm) and contact angle of 0° gives $h_{max}$ of 430 mm which is double the measured height obtained in the experiment. However by increasing the contact angle to 66° the calculated maximum height of water matches the measured value of 217 mm. Although the simpler estimate given by Eq. (1) will be adopted here, avoiding the many assumptions necessary in the application of Eq. (2), it will be found below that a large value of contact angle $\alpha$ will similarly need to be invoked to marry predictions and measurements.

## 5. Discussion

In contrast to the single estimate of capillary rise provided by Eq. (1), the disposition of water found in Fig. 8 and Fig. 11 suggests a diversity of regimes, but not precisely those offered from drying tests and idealised in Fig. 1. In the absence either of any history of wetting and drying, or of any temperature cycling, it is unreasonable to expect any pendular moisture zone III of isolated droplets since there is no plausible transport mechanism to explain their presence. The extent of fluid rise shown by Eq. (2), can create a situation whereby the water will rise higher that the saturated capillary fringe. On the other hand, Eq. (1) offers a prediction of capillary rise that depends directly on pore size. Further analysis is necessary to explain the distribution of fluid within the unsaturated zone. Across rough grain surfaces, pendular fluid distributions can be hydraulically connected by thin films (Davis et al., 1990) but in the dry surface environment, which is maintained in these experiments, surface films are likely to be short lived once the fluid has reached its maximum capillary rise height. Wetting front instability is likely to be present given that the sand is dry and the possible change in fluid properties at the air boundary leading to infiltration of fluid fingers (Wang et al., 1998) as the water seeps upwards. Further experiments to define the SWCC following the capillary rise into various dry soils would enable a similar statistical analysis of curve-fitting functions as already employed by Zhai and Rahardjo (2013) on the drying of initially saturated soils. The salient difference would be a sharp transition into dry soil above the rising capillary zone, as seen in Figs. 7, 8 and 11 above, rather than the exponential tail of residual water seen on the drying branch of existing SWCC data.

The evidence following the wetting of initially dry sand from below suggests the development of the following zones:

(i) Immediately above the water table, a quasi-saturated zone (Faybishenko, 1995) is found (S > 0.8 in the experiments described here) which may be thought of as a saturated matrix but with its larger voids accommodating occasional air bubbles. Such bubbles could be trapped by water rising faster in the tighter pore spaces between surrounding strings of finer grains. It would appear from Fig. 8 and 11 that the maximum elevation of this zone above the water table in Fraction D sand in the laboratory experiments was 130 mm ± 20 mm at 20 °C and 110 mm ± 10 mm at 35 °C.

(ii) Above the quasi-saturated capillary zone, a zone of funicular fingering forms by water percolating upwards in increasingly narrow channels defined by grains smaller than $D_{10}$, by the contact zones of other grains, and by the encroaching atmospheric air that surrounds them. It appears from Fig. 8 and 11 that the maximum elevation of this zone above the water table in the laboratory experiments was 238 mm ± 10 mm at 20 °C and 217 mm ± 20 mm at 35 °C.

The applicability of Eq. (1) to the depth of these zones is not immediately obvious. However, pressures within the continuous water phase of the quasi-saturated zone (i) must ultimately achieve a hydrostatic equilibrium consistent with the unit weight of pure water and the net effect of capillary suction at the (i)-(ii) boundary. However, unless

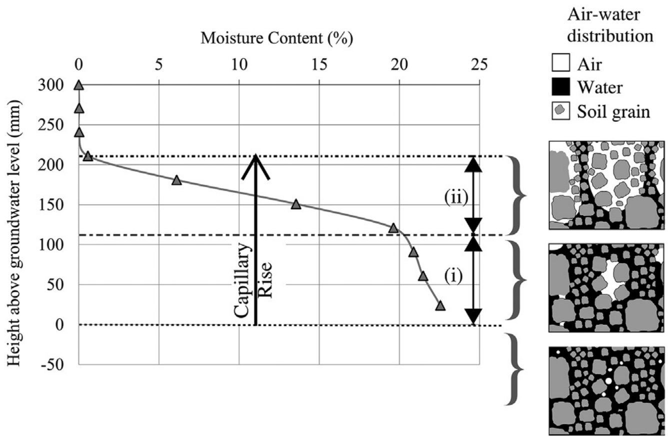


**Fig. 12.** Suggested elements of the vadose zone for water rising into dry sand.

rising head tests of the sort described here are carried out on the sand of interest, there will remain some uncertainty regarding the appropriate grain size fraction to characterise the equivalent pore diameter d, and the value to be taken for the contact angle α.

According to Culligan et al. (2005) contact angles of water on apparently dry, clean silica sand can be as high as 58°, possibly due to unrecognised surface contamination. Liu et al. (2016) showed that contact angle can also be influenced by other properties such as surface roughness and pore diameter and measured contact angles up to 63°. Even higher contact angles were determined by Malik et al. (1984) between water and dry glass beads.

To support the current investigation, measurements of capillary height were obtained using 0.8 mm diameter borosilicate glass tubes. Correspondingly, it was found that unless the bores were chemically cleaned, the capillary height was substantially reduced. If the top of the capillary fringe at 35 °C is taken as 110 mm (see Fig. 11) and the contact angle is taken as zero, the equivalent pore diameter using Eq. (1) for the quasi-saturated capillary zone is given as 0.26 mm. A contact angle of 44° in the present study avoids the factor 0.7 error which would otherwise exist between Eq. (1) and the observed height of the saturated capillary zone, if the equivalent pore diameter is to match $D_{10}$ = 0.19 mm, the grain size of the Fraction D sand. The circa 110 mm deep quasi-saturated capillary zone therefore appears to be predictable using $D_{10}$ and Young-Laplace, only if there is assumed to be imperfect wetting of the rising water against the dry sand grains. Accepting that the unsaturated funicular moisture zone extends a further 107 mm, with a maximum capillary rise of 217 mm, the use of Eq. (1) requires that the equivalent pore diameter in the smallest pores be reduced to $0.52D_{10}$. It is quite consistent with our understanding of funicular fingering to consider that larger pores which remain air-filled are irrelevant to the passage of water in the smallest pores which take their apertures from the $D_{10}$ grains that surround them.

In many applications, the unsaturated zone of capillary fingering may have a significant effect. In the experiments reported here this zone extends to an elevation above the water table of 217 mm, or about double the extent of the quasi-saturated capillary zone. It would clearly be proper to take this extended region into account in assessments of the rate of groundwater seepage, the spread of pollution, or the impact of dissolved salts on engineering foundations (Hird and Bolton, 2016). In the field, subject as it is to wetting and drying cycles, there may also exist an upper region of pendular water at very low degrees of saturation, wherein transport can only occur by vapour diffusion. A revised suggestion for zones of moisture in relation to the groundwater table, respecting the capillary mechanisms that have been inferred, is sketched in Fig. 12.

This work proposes in Fig. 12 a new arrangement of water and air phases appropriate to the upward percolation of groundwater, whereas Fig. 1 showed the currently conventional view derived from downward seepage of previously saturated soil. Its significance goes beyond the well-known distinction between the drying and wetting branches of the SWCC, however. The present work also emphasises the potential significance of the atmospheric boundary condition, in terms of relative humidity. The distribution of pendular water in Fig. 1 would eventually evaporate if the atmosphere possessed RH < 100%. But it has been shown that the capillary water existing as continuous funicular threads in the unsaturated vadose zone can be maintained by upward seepage even if it is being slowly depleted by evaporation.

## 6. Conclusion

This paper describes an experiment examining the capillary rise height of water through columns of initially dry sand. Flow columns containing dry medium grained sand were stood in a shallow tray of deionised water and with the sand surface exposed and showed that fluid was able to travel further than theoretical estimates. The experiments were purposely set up with dry air above the sand column, recognising that this would militate against the formation of any isolated pendular droplets. The presence of water in the sand was determined by gravimetric sampling and through the use of TDR probes. It was found that despite a temperature increase and reduction in relative humidity of the air at the surface, fluid extended well above the saturated capillary fringe to create an unsaturated capillary fringe. Although theoretical estimates of fluid height above the capillary fringe have been determined by others using soil properties including hydraulic conductivity, Young-Laplace is still relevant for determining capillary height so long as pore variability and fluid contact angle with the dry surface are taken into account. Funicular fingering is responsible for fluid transport through pores (smaller than $D_{10}$) above a zone considered to be quasi-saturated. TDR probes are capable of measuring the funicular rise of fluid beyond the saturated capillary fringe so that empirical evaluations need not be conducted. This preliminary study challenges the conventional understanding of capillary rise in unsaturated soil subjected to rapid evaporation, but a further study with other porous media is recommended.

## References

Bear, J., 1972. Dynamics of fluids in porous media. Dover Publications, Inc. New York.
Carman, P.C., 1937. Fluid flow through granular beds. Trans. Inst. Chem. Eng. 15, 150–166.
Culligan, P.J., Ivanov, V., Germaine, J.T., 2005. Sorptivity and liquid infiltration into dry soil. Adv. Water Resour. 28 (10), 1010–1020. http://dx.doi.org/10.1016/j.advwatres.2005.04.003.
Davis, T.H., Novy, R.A., Scriven, L.E., Toledo, P.G., 1990. Fluid distribution and transport in porous media at low wetting saturations. J. Phys. Condens. Mat. 2, SA457–SA464. http://dx.doi.org/10.1088/0953-8984/2/S/073.
Faybishenko, B.A., 1995. Hydraulic behaviour of quasi-saturated soils in the presence of entrapped air: Laboratory experiments. Water Resour. Res. 31 (10), 2421–2435. http://dx.doi.org/10.1029/95WR01654.
Feia, S., Ghabezloo, S., Bruchon, J.-F., Sulem, J., Canou, J., Dupla, J.-C., 2014. Experimental evaluation of the pore-access size distribution of sands. Geotech. Test. J. 37 (4), 1–8. http://dx.doi.org/10.1520/GTJ20130126.
Fredlund, D.G., Rahardjo, H., 1993. An overview of unsaturated soil behaviour. In: Proceedings of ASCE Speciality Series on Unsaturated Soil Properties, pp. 1–31 October 24–28. (Dallas, TX).
Haines, W.B., 1930. Studies in the physical properties of soil. V. The hysteresis effect in capillary properties, and the modes of moisture distribution associated therewith. J. Agric. Sci. 20 (01), 97–116. http://dx.doi.org/10.1017/S002185960008864X.
Hird, R., Bolton, M.D., 2016. Migration of sodium chloride in dry porous materials. In: Proceedings of the Royal Society A. 472. pp. 2186. http://dx.doi.org/10.1098/rspa.2015.0710.
Jones, S.B., Wraith, J.M., Or, D., 2002. Time domain reflectometry measurement principles and applications. Hydrol. Process. 16, 141–153. http://dx.doi.org/10.1002/hyp.513.
Krisdani, H., Rahardjo, H., Leong, E.C., 2008. Measurement of geotextile-water characteristic curve using capillary rise principle. Geosynth. Int. 15 (2), 86–94. http://dx.doi.org/10.1680/gein.2008.15.2.86.
Lehmann, P., Gambazzi, F., Suski, B., Baron, L., Askarinejad, A., Springman, S.M., Holliger, K., Or, D., 2013. Evolution of soil wetting patterns proceeding a hydrologically induced landslide inferred from electrical resistivity survey and point

measurements of volumetric water content and pore water pressure. Water Resour. Res. 49, 7992–8004. http://dx.doi.org/10.1002/2013WR014560.

Liu, Q., Yasufuku, N., Miao, J., Ren, J., 2014. An approach for the quick estimation of maximum height of capillary rise. Soils Found. 54 (6), 1241–1245. http://dx.doi.org/10.1016/j.sandf.2014.11.017.

Liu, Z., Yu, X., Wan, L., 2016. Capillary rise method for the measurement of the contact angle of soils. Acta Geotech. 11, 21–35. http://dx.doi.org/10.1007/s11440-014-0352-x.

Lucas, D.R., Askarinejad, A., Herzog, R., Bleiker, E., Springman, S.M., 2015. Volumetric water content determination by TDR sensors and decagons in gravelly soils. In: ICE Publishing Conference Proceedings: Investigation, Classification, Testing, and Forensics. 116. pp. 3565–3570. Chapter. https://doi.org/10.1680/ecsmge.60678.

Malik, R.S., Kumar, S., Dahiya, I.S., 1984. An approach to the quick determination of some water transmission characteristics of porous media. Soil Sci. 137 (6), 395–400.

Robert, D., Soga, K., 2010. Soil-pipeline interaction in unsaturated soils. In: Laloui, L. (Ed.), Mechanics of Unsaturated Geomaterials. John Wiley & Sons, Inc., NJ, pp. 303–325.

Silliman, S.E., Berkowitz, B., Simunek, J., Genuchten, M.T., 2002. Fluid flow and solute migration within the capillary fringe. Ground Water 40 (1), 76–84. http://dx.doi.org/10.1111/j.1745-6584.2002.tb02493.x.

Tanaka, M., Girard, G., Davis, R., Peuto, A., Bignell, N., 2001. Recommended table for the density of water between 0C and 40C based on recent experimental reports. Metrologia 38, 301–309. http://dx.doi.org/10.1088/0026-1394/38/4/3.

Terzaghi, K., Peck, R.B., 1964. Soil mechanics in engineering practise. Wiley, New York.

Topp, G.C., Davis, J.L., Annan, A.P., 1980. Electromagnetic determination of soil water content: measurement in coaxial transmission lines. Water Resour. Res. 16 (3), 574–582. http://dx.doi.org/10.1029/WR016i003p00574.

Van Genuchten, M.T., 1980. A closed-form equation for predicting the hydraulic conductivity of unsaturated soils. Soil Sci. Soc. Am. J. 44, 892–898.

Vargaftik, N.B., Volkov, B.N., Voljak, L.D., 1983. International tables of the surface tension of water. J. Phys. Chem. Ref. Data 12 (3), 817–820. http://dx.doi.org/10.1063/1.555688.

Venard, J.K., Street, R.L., 1975. Elementary Fluid Mechanics, 5th ed. Wiley, New York.

Wang, Z., Feyen, J., Elrick, D.E., 1998. Prediction of fingering in porous media. Water Resour. Res. 34 (9), 2183–2190.

Yang, H., Rahardjo, H., Leong, E.-C., Fredlund, D.G., 2004. Factors affecting drying and wetting soil-water characteristic curves of sandy soils. Can. Geotech. J. 41, 908–920. http://dx.doi.org/10.1139/t04-042.

Zhai, Q., Rahardjo, H., 2013. Quantification of uncertainties in soil-water characteristic curve associated with fitting parameters. Eng. Geol. 163, 144–152. http://dx.doi.org/10.1016/j.enggeo.2013.05.014.